ISSN: 3068-1774
Review Article

Journal of Material Sciences & Applied Engineering

Lubricant Feeding Environment and Enhancement with Reducing Friction

Rakesh ManilalPatel[1], Pragna A. Vadher[2], Gunamani B Deheri[3], Sanjay Chaudhary[4], Dhinesha Ruwanthi Perera[5] & Ajmeera Chandulal[6]

[1]*Department of Mathematics, Government Science College, Gandhinagar India*
[2]*Principal, Government Science College, Idar, India*
[3]*Retired Asso. Prof. of Mathematics, Dept. of Maths, S. P. Univ., V. V. Nagar, India.*
[4]*Dept. of Mathematics, IBS, DRBAU, Agra, India.*
[5]*Senior lecturer, GSJKD University, Sri Lanka.*
[6]*Asst. Prof., Dept. of Maths, National Sanskrit University, Tirupati, India*

***Corresponding author:** Rakesh Manilal Patel, Department of Mathematics, Government Science College, Gandhinagar India. Ph No: +91 9426530263.

Submitted: 17 September 2025 **Accepted:** 25 September 2025 **Published:** 30 September 2025

https://doi.org/10.63620/MKJMSAE.2025.

Citation: *Patel, R. M., Vadher, P. A., Deheri, G. B., Chaudhary, S., Perera, D. R., & Chandulal, A. (2025). Lubricant Feeding Environment and Enhancement with Reducing Friction. J Mat Sci Apl Eng, 4(5), 01-12.*

Abstract

The performance of hydrodynamic journal bearings is significantly influenced by the conditions under which the lubricant is supplied. However, many existing studies tend to overlook these factors, often generalizing their impact on bearing performance. This article presents a comprehensive thermo-hydrodynamic analysis that takes lubricant supply conditions into account. The study involves a numerical solution of the generalized Reynolds equation, along with the energy equations governing the lubricant film and heat transfer within the bearing bush. Special attention is given to the phenomena occurring within and around the grooves, as well as in regions where the lubricant film experiences rupture. The investigation assesses the effects of various variables, including lubricant feed pressure, temperature, groove length ratio, groove width ratio, and the number of grooves (single or twin), on bearing performance across a wide range of conditions. The results are consistent with existing experimental data, validating the accuracy of the model in capturing these phenomena. The study concludes that optimizing lubricant supply conditions can significantly enhance bearing performance.

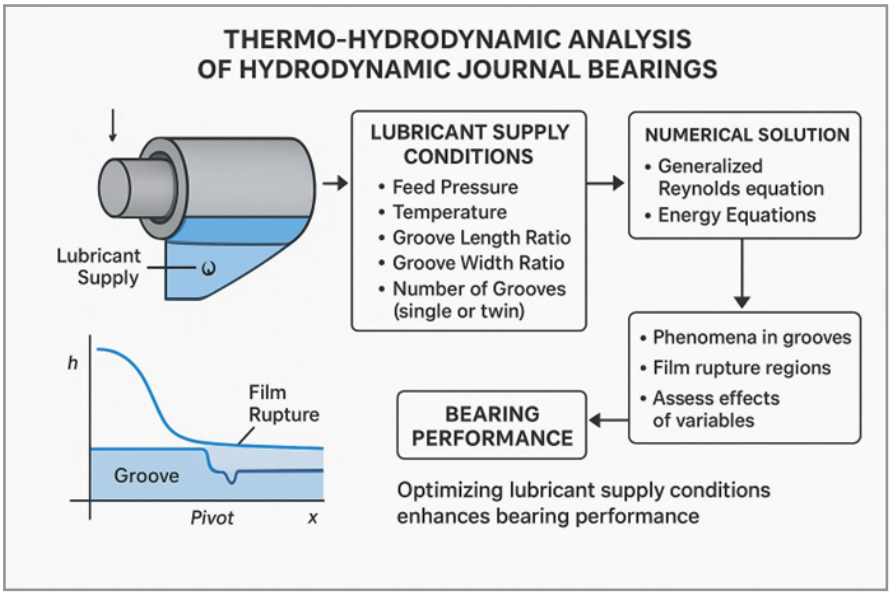

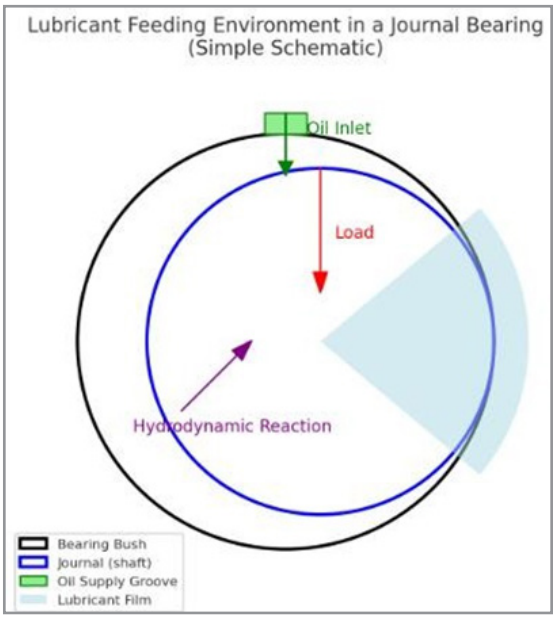

Journal Bearing Showing the Lubricant Feeding Environment:
Outer circle (black): Bearing bush
Inner circle (blue): Journal (shaft)
Green Slot + Arrow: Oil supply groove & inlet
Blue Shaded Wedge: Lubricant film forming the hydrodynamic wedge,
Red arrow: Applied load, Purple Arrow: Hydrodynamic reaction force.

Keywords: Reynolds Equation (re), Deformable Roughness (dr), Feeding Conditions (fc), Thermo Hydrodynamic Model (thm), Pressure Profile (pp), Load Carrying Capacity (lcc), Friction.

Subject Classification
74A55 Theories of friction (tribology); 74Dxx Materials of strain-rate type and history type, other materials with memory (including elastic materials with viscous damping, various viscoelastic materials); 00A69 General applied mathematics {For physics, see 00A79 and Sections 70 through 86} 00A71 Theory of mathematical modeling 00A72 General methods of simulation.

Literature Review and Introduction

The accurate prediction of hydrodynamic journal bearing behavior is far more complex than its seemingly simple geometry might suggest. This complexity arises from the need to simultaneously account for pressure, flow, and heat transfer while incorporating phenomena such as film rupture, dual-phase flow, film reformation, forced and free convection, viscous dissipation, inner groove lubricant flow mixing, and thermoelastic distortion. Developing an integrated model that effectively addresses all these factors while maintaining acceptable computation times is challenging. Consequently, oversimplified models have often been employed. In particular, the incorporation of lubricant feeding conditions has frequently been simplified or entirely neglected in many theoretical approaches. This oversight-such as ignoring the effects of feeding pressure, feeding temperature, or groove geometry-may explain the notable discrepancies often observed between theoretical predictions and experimental results. These discrepancies are especially pronounced in twin-groove journal bearings, where experimental data on lubricant feeding conditions are scarce. This lack of experimental focus has contributed to the underappreciation of the critical role that feeding conditions play in bearing performance. Incorporating realistic lubricant feeding conditions into journal bearing analyses introduces theoretical challenges, depending on the model used. Many models simplify or exclude feeding conditions, relying on approaches such as:

- Assuming full film reformation at the position of maximum film thickness or the groove location [1].
- Modeling grooves with infinitesimal width and no circumferential extension [2,3].
- Extending grooves of finite width to the full length of the bush body [4-6].
- Treating finite-size grooves by imposing flow rate or assuming no feeding pressure (ambient conditions) [5].
- Neglecting or oversimplifying thermal phenomena in the groove region, such as recirculated hot oil, feeding temperature, reverse flow (oil re-entering the groove from downstream), or backflow (fresh oil flowing upstream).

Some studies have attempted to address the influence of lubricant feeding conditions. For instance, used a finite element method (FEM) analysis with a 1D energy equation and modeled axial pressure profiles using second-order polynomials [7]. They demonstrated that feeding pressure reduces maximum temperature, particularly at low Sommerfeld numbers, while increasing flow rate and slightly affecting power loss. Theoretical and experimental investigations on high-speed twin-groove journal bearings, as reported in, explored the influence of groove position relative to load direction [8,9]. A more rigorous thermo hydrodynamic (THD) approach was used in these studies, incorporating viscosity and temperature variations through the film thickness, heat conduction in solid components, and a groove mixing model for inlet temperature calculation. This approach significantly improved the agreement between theoretical predictions and experimental temperature profiles, although discrepancies in flow rate remained. Attention to film reformation and mass- conserving algorithms for feeding conditions was highlighted by [10]. A

comprehensive theoretical and experimental analysis of circular journal bearings with various groove configurations, including twin axial grooves, was conducted by [11].

Using a mass- conserving algorithm proposed by, they showed that neglected parameters, such as feeding pressure and groove geometry, significantly affect bearing performance [12]. This approach was later extended to account for thermal effects and validated with experimental evidence [13, 14]. Other researchers, such as Ma and Taylor, examined the effects of feeding pressure and temperature on twin-groove elliptical bearings [15].

They found that increasing feeding temperature significantly raised maximum temperatures and flow rates while reducing power loss. Conversely, higher feeding pressure increased flow rate while moderately reducing bush temperatures and power loss.The impact of lubricant starvation on THD performance was explored by, demonstrating that proper groove placement could reduce flow rate and power loss without compromising load capacity [18]. Additional work on circumferentially grooved journal bearings emphasized the importance of explicitly incorporating groove pressure and entry temperature into the energy equation to account for mixing effects.Despite these efforts, experimental investigations on twin-groove journal bearings remain limited, particularly regarding the effects of varying feeding conditions and their optimization to enhance performance [20]. Recent studies by the authors aimed to address this gap by examining the impact of feeding pressure and temperature on a 100mm twin axial groove bearing [24]. Results showed that increased feeding pressure significantly raised oil flow rates, with minimal impact on maximum temperature and power loss except for lightly loaded bearings. Shaft temperature was observed to align closely with maximum bearing temperature under low loads but was significantly lower under high loads. Further experimental work on a 50mm twin axial groove bearing revealed the importance of measuring individual groove flow rates [25].

Findings showed that downstream grooves provided minimal cooling under low eccentricities but became more effective as eccentricity increased, while upstream grooves exhibited the opposite behavior. Negative flow rates in upstream grooves under high loads and low feeding pressures were found to dramatically affect performance. In addition, comparisons of single- groove and twin-groove configurations highlighted that under heavy loads, twin grooves could deteriorate performance due to uneven lubricant feed [27]. These results suggest that knowledge of individual groove flow rates can inform strategies such as groove deactivation or flow balancing to optimize performance. Building on this, the authors investigated the effect of groove angle on flow rates in twin-groove bearings, noting that increasing the groove angle decreased upstream flow rates while increasing downstream flow rates [28]. Reverse flow phenomena were observed in both grooves under certain conditions.This study presents a thermo hydrodynamic (THD) model for hydrodynamic journal bearings, with a focus on twin-groove configurations.

The model integrates realistic feeding conditions, including groove geometry and lubricant properties, and employs mass and energy-conserving algorithms. It also incorporates models for film rupture and reformation, lubricant mixing, and thermoelastic effects. Following a thorough validation against experimental data, the study conducts an extensive parametric analysis of lubricant feeding conditions, such as pressure, temperature, groove dimensions, and groove number (single vs. twin), to assess their impact on bearing performance. The findings aim to provide a deeper understanding of the mechanisms affecting journal bearing performance, with particular attention to twin-groove configurations where theoretical prediction discrepancies are most pronounced.

Mathematical and Theoretical Model

The theoretical model for analyzing the steady-state performance of journal bearings, particularly with regard to lubricant feed conditions, builds upon earlier isoviscous and thermo hydrodynamic (THD) models developed by the research group [11,13]. While many aspects of the model have been thoroughly detailed in previous studies, especially in, this description provides a concise overview [13].

The model incorporates a comprehensive THD analysis and accounts for lubricant feed conditions, including feeding pressure, temperature, and specific groove dimensions. By using input data such as the physical properties of the lubricant and bearing components, operating conditions, geometric configurations, and lubricant feed parameters, the model aims to generate essential performance metrics for bearing design and evaluation. These metrics include hydrodynamic pressure and temperature distributions, oil flow rate, minimum film thickness, eccentricity, attitude angle, shaft torque, and power loss. Figure A illustrates the bearing geometry, highlighting key geometric features.

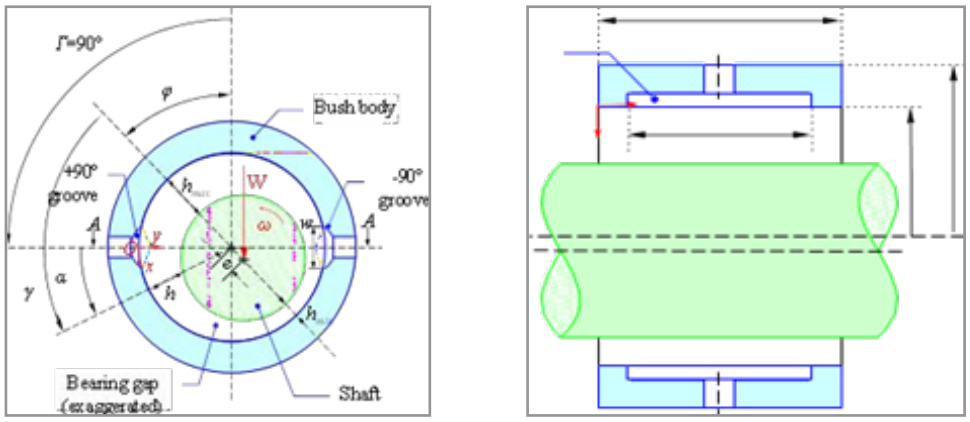

Figure A : Bearing geometry

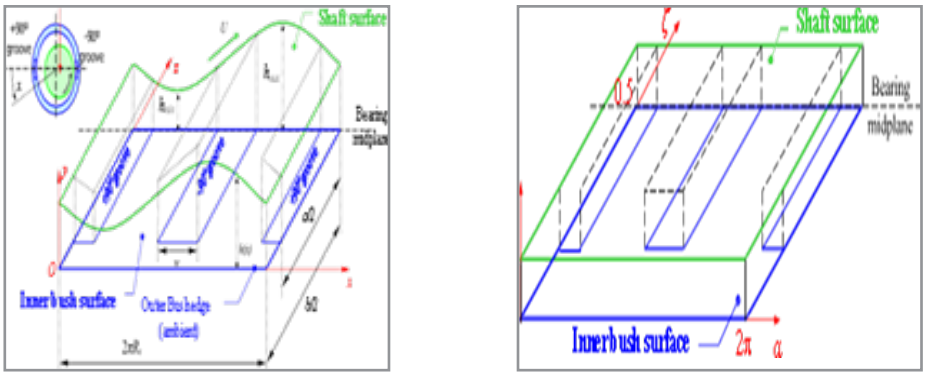

Figure B: Dimensionless (normalized) fluid domain non wrapped\dimensional, Brito FP, et. al., 2014.

Figure B presents the unwrapped bearing gap geometry along with the corresponding axis system, presented in both dimensional and non-dimensional normalized forms. This representation is based on the reasonable assumption that the effects of bearing curvature and inertia can be neglected.

Pressure and velocity Fields

The calculations for the pressure and flow fields are based on several widely accepted assumptions. These include the following:

Thin Film Approximation: Pressure is assumed to be uniform across the film thickness, except in groove regions where this assumption is not valid.

Laminar Flow: The flow is considered laminar, with viscous effects dominating over fluid inertia and gravitational forces.

- **Steady-State Regime:** The system is assumed to operate under steady-state conditions.
- **Fluid Properties:** The fluid is assumed to be incompressible and Newtonian, with its viscosity dependent solely on temperature.
- **Negligible Bearing Curvature Effects:** The effect of bearing curvature is considered negligible, as the clearance is much smaller than the bearing radius.
- **No Surface Contact or Roughness:** There is no contact between surfaces, and the surface roughness is negligible, resulting in a hydraulically smooth surface in the fully hydrodynamic regime.
- **Thermal Expansion:** Thermal expansion of the components is assumed to be uniform and is based on their average temperature, influencing only their diameter in a differential thermal expansion approach.

The hydrodynamic pressure field, P(x,z) is governed by the Generalized Reynolds Equation (GRE), which is derived from a flow balance [29].

$$\underbrace{\frac{\partial}{\partial x}\left[\rho_l F_2 \frac{\partial p}{\partial x}\right]}_{Duetopoiseuilleflow} + \underbrace{\frac{\partial}{\partial z}\left[\rho_l F_2 \frac{\partial p}{\partial z}\right]}_{DuetoaxialFlow} = U \underbrace{\frac{\partial}{\partial x}\left[\rho_l h F_3\right]}_{DuetoCoueteflow} \quad (1)$$

With The Viscosity Integrals, Which Account for Cross-Film Viscosity Variation, Being Defined as Follows:

$$F_0 = \int_0^h \frac{1}{\mu_l} dy;\ F_1 = \int_0^h \frac{y}{\mu_l} dy;\ F_2 = \int_0^h \frac{y}{\mu_l}\left(y - \frac{F_1}{F_0}\right) dy;\ F_3 = 1 - \frac{F_1}{hF_0} \quad (2)$$

The standard solution for equation (1) is applicable only in the full film region, where pressure is greater than ambient (P > 0). In low-pressure conditions, such as sub-ambient scenarios, the lubricant cannot maintain a continuous film and instead separates into discrete streamlets, separated by gaseous cavities, with pressure assumed to be uniform and equal to ambient. Therefore, a suitable algorithm is required to identify the boundaries of the ruptured film region and to apply specific treatments in that area. The rupture boundary can be determined using the Reynolds condition, which considers both pressure and pressure gradients in the direction of bearing rotation to be zero. This condition ensures flow continuity and is widely accepted in bearing modeling. Regarding the film reformation boundary condition, some authors simplify the assumption by placing it at the position of maximum film thickness or at the circumferential coordinates of grooves, which are considered to have negligible thickness and to extend the full length of the bearing. However, this approach imposes a specific location for film reformation rather than providing a reliable method for estimating it, which is inadequate for realistic feeding conditions, the focus of this work. In reality, film reformation occurs when the bearing gap is locally filled with lubricant at the circumferential location where the recirculated flow volume is sufficient to fill the gap. This can be computed based on an understanding of flow patterns and continuity.

The General Reynolds Equation (GRE) fundamentally computes flow continuity by accounting for various flow components within the bearing gap. Under the simplifying assumptions mentioned, these flows are reduced to pressure-driven flow (Poiseuille) and drag-driven flow (Couette). In the ruptured film region, pressure is typically considered ambient, resulting in purely drag- driven flow. Consequently, mass flow continuity can be easily computed, allowing for the identification of the film reformation boundary. To achieve this, the GRE can be modified in the ruptured film region to create a mass-conserving equation that is valid throughout the entire bearing domain. This approach was implemented by the algorithm proposed by Elrod, which is based on a mass balance of Couette and Poiseuille flows across a finite control volume surrounding each computational node [12].

Poiseuille and Couette flow calculations are performed in the full film region, while Couette flow and liquid fraction are accounted for in the ruptured film region. A substitution variable, utilizing a switch function that takes a value of 0 or 1 depending on whether the film is ruptured (P = 0) or intact (P > 0), is employed for this purpose. The result is a mass-conservative finite difference version of the Reynolds equation, valid across

the entire domain, and solved iteratively using the Gauss-Seidel method, with the switch function updated at each iteration.This work utilizes the adapted algorithm for thermal hydrodynamics (THD) developed by Costa et al. [13]. A key advantage of this method is its automatic provision of mass flow rates for lubricant crossing all faces of each computational cell, along with the corresponding local liquid fraction in the ruptured film region.

This feature is particularly useful for calculating flow rates at critical points, such as groove edges, which is essential for analyzing feeding conditions and for incorporating into thermal models of ruptured film regions based on effective length concepts as described in [4]. Additionally, the velocity field must be computed, as it influences the convective and dissipative terms of the energy equation. The expressions for the circumferential and axial components of velocity are the sum of the Poiseuille and Couette components, accounting for variable viscosity [29].

$$u_x = \frac{\partial p}{\partial x}\left\{F_4 - \frac{F_1 F_5}{F_0}\right\} + U\frac{F_5}{F_0} \tag{3.a}$$

$$u_z = \frac{\partial p}{\partial z}\left\{F_4 - \frac{F_1 F_5}{F_0}\right\} \tag{3.b}$$

With

$$F_4 = \int_0^y \frac{\lambda}{\mu_l}\, d\lambda \tag{3.c}$$

$$F_5 = \int_0^y \frac{1}{\mu_l}\, d\lambda \tag{3.d}$$

being λ a dummy variable of y. The radial velocity uy is obtained from the solution of the flow continuity equation computed solely for the liquid portion of the flow, which must be affected by the local liquid fraction, θ*:

$$\frac{\partial(\theta^* u_x)}{\partial x} + \frac{\partial(\theta^* u_y)}{\partial y} + \frac{\partial(\theta^* u_z)}{\partial z} = 0 \tag{4}$$

Basic Thermal Model

The thermal problem is coupled with the flow problem because viscous dissipation is influenced by velocity gradients, while the pressure and velocity fields are affected by viscosity, which is temperature-dependent.

- Fluid Domain: In this region, the energy equation is solved.
- Bush Body Domain: Here, the Laplace equation governs conductive heat transfer.
- Groove Regions: In these areas, the Reynolds equation is not applicable (the thin film condition does not hold). Only mass and energy balances are performed in this domain.

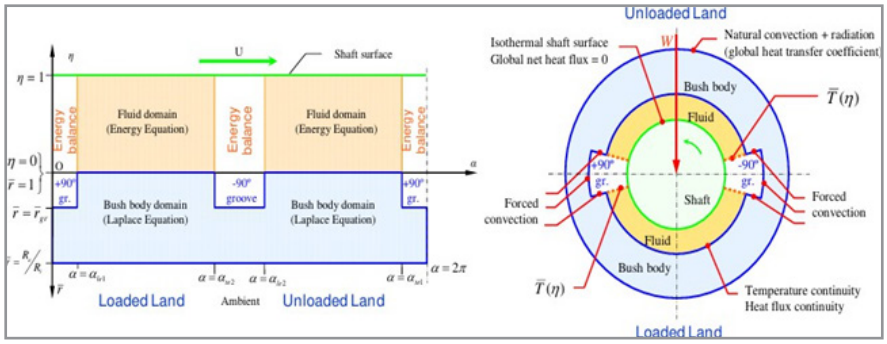

Figure C: Calculation Domains and Boundary Conditions Used in the Thermal Model

Figure C: Outline of the calculation domains and boundary conditions used in the thermal model Some of the simplifying assumptions include: absence of axial temperature gradients (calculations are performed in the midplane only); the circumferential and axial diffusive terms may be neglected when compared with the corresponding convective terms (high Peclet number), which leads to purely radial conductive heat transfer; Only dissipative terms based on transverse gradients are relevant; The bearing is perfectly aligned – i.e. axial symmetry is assumed. Fluid domain the aforementioned assumptions lead to the following simplified form of the energy equation at the midplane of the bearing [29]:

$$\underbrace{(\rho c_p)_{eq}\left[u_x\frac{\partial T}{\partial x} + u_y\frac{\partial T}{\partial y}\right]}_{\text{convective term (convection)}} = \underbrace{K_{eq}\frac{\partial^2 T}{\partial y^2}}_{\text{diffusive term (conduction)}} + \underbrace{\mu_{eq}\left(\frac{\partial u_x}{\partial y}\right)^2}_{\text{dissipative term (heat generation)}} \tag{5}$$

(ρcp) eq and Keq are the properties (density, specific heat and thermal conductivity) of the lubricant or the equivalent properties or the lubricant streamers plus gaseous cavities at the ruptured film region. These will depend on the specific modelling of the ruptured film region. It is common to use the "Effective Length" concept to model the ruptured film region [4]. In fact, if both the lubricant streamers and the gaseous cavities are attached to the bush and shaft surfaces and considering heat transfer to occur radially and in parallel through liquid and gaseous streamers, it may be proved that the equivalent physical properties of the liquid plus gas mixture will be an average of the liquid and gas properties weighted by their corresponding fraction in the mixture, with a particularity found by the authors in which the density and specific heat should be treated as a group, as seen in (1). The effective fraction of the bearing length which is filled with liquid lubricant is therefore called the effective length of lubricant, EL, easily computed by integrating the fluid fraction along the relevant section. The equivalent properties will therefore be the following:

$$\begin{cases} (\rho C_p)_{eq} = \overline{EL}\cdot\rho_l c_{p_l} + \left(1-\overline{EL}\right)\cdot\rho_g C_{p_g} \\ K_{eq} = \overline{EL}\cdot K_l + \left(1-\overline{EL}\right)\cdot K_g \\ \mu_{eq} = \overline{EL}\cdot\mu_l + \left(1-\overline{EL}\right)\cdot\mu_g \end{cases} \tag{6}$$

Only be valid for the thermal calculations (they have been derived based on the energy equation). The properties used for the pressure and flow calculations will be solely based on those of the liquid portion of the flow. There is experimental evidence

that in the ruptured film region not all the lubricant flows along streamers that are attached to both the shaft and bush surfaces. In reality, a portion of it is attached solely to the shaft surface forming an adhered layer to this surface [31]. This will affect heat transfer since no velocity gradients (and therefore no heat dissipation) will be present for that portion of the lubricant. Some authors have taken this phenomenon into account, although within the scope of a simplified model [4].

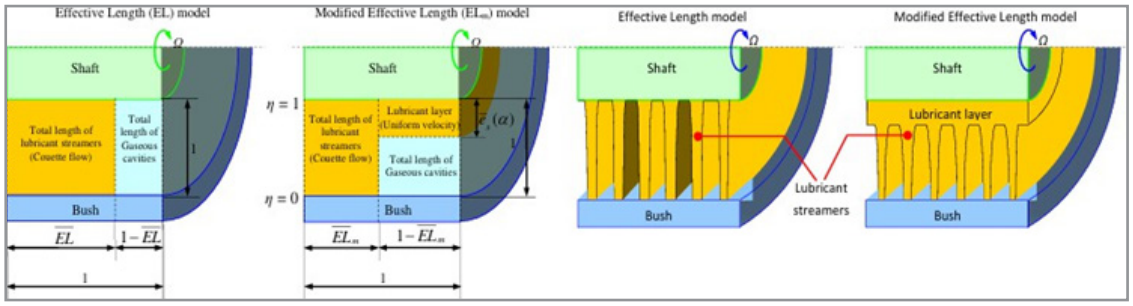

Figure D: Comparison between the Effective Length and the modified Effective Length thermal models of the ruptured film region proposed in the present work. The following expressions for the equivalent properties for thermal calculations, which will vary according to the radial position in the film (whether in the layer region or the streamer-only region) have been derived:

$$\text{Streamer-only region } \left(0 \le \eta < 1-\bar{e}_s(\alpha)\right) \qquad \text{Layer region } \left(1-\bar{e}_s(\alpha) \le \eta \le 1\right)$$

$$\begin{cases} \left(\rho C_p\right)_{eq} = \overline{EL}_m \cdot \rho_l c_{p_l} + \left(1-\overline{EL}_m\right) \cdot \rho_g C_{p_g} \\ K_{eq} = \overline{EL}_m \cdot K_l + \left(1-\overline{EL}_m\right) \cdot K_g \\ \mu_{eq} = \overline{EL}_m \cdot \mu_l + \left(1-\overline{EL}_m\right) \cdot \mu_g \end{cases} \qquad \begin{cases} \left(\rho C_p\right)_{eq} = \rho_l c_{p_l} \\ K_{eq} = K_l \\ \mu_{eq} = \overline{EL}_m \cdot \mu_l \end{cases} \tag{7}$$

With m EL being the corrected Effective Length of lubricant, which corrects EL in order to reflect the portion of lubricant which has been taken out of streamer flow (Couette flow) and allocated to the shaft adhered layer (uniform flow).) (s e is the fraction of the bearing gap occupied by the lubricant layer at a given circumferential position α, calculated by continuity from its initial value at the rupture front, 0 s e, and the variation of the local film height,) (h:

$$\overline{EL}_m = \frac{\overline{EL} - 2\bar{e}_s(\alpha)}{1-2\bar{e}_s(\alpha)} \qquad \bar{e}_s(\alpha) = \bar{e}_{s0} \cdot \frac{\bar{h}(\alpha_{rupt})}{\bar{h}(\alpha)} \tag{8}$$

It may be easily deduced that if all the lubricant will flow adhered to the shaft with no streamers present (mEl = 0), the fraction of the bearing gap occupied by the lubricant layer will be at the best 0.5 (the linear profile of the Couette flow of the streamers will be converted into a uniform velocity profile possessing the speed of the shaft) and no heat dissipation will occur. Again, the existence of this shaft-adhered layer has been considered only for the thermal model. The computation of cell flow rates which is the basis for the pressure field calculation relies on the assumption that in the ruptured film region the lubricant flows solely along streamers attached both to the bush and the shaft surfaces. The energy equation is solved through a method proposed by, which consists in solving the energy equation as an initial value problem in the circumferential direction [3]. This may be done as long as the circumferential velocity component is positive. However, if a region with negative speed exists, then this solution scheme may still be applied using the domain separation iterative approach, where calculations are performed successively in the two separate speed domains (positive and negative) as an initial value problem and in the direction of the flow. The results of one domain will be used as a boundary/initial condition for the other one.

Bush Body Domain

The conductive heat transfer across the bush body is solved through the Laplace Equation for cylindrical coordinates [29].

$$\frac{\partial^2 T_b}{\partial r^2} + \frac{1}{r}\frac{\partial T_b}{\partial r} + \frac{1}{r^2}\frac{\partial^2 T_b}{\partial \alpha^2} = 0$$

is the two-dimensional Laplace equation in polar coordinates. Use separation of variables $T_b(r,\alpha) = R(r)\Theta(\alpha)$. Substituting and dividing by $R\Theta$ gives

$$\frac{r^2R'' + rR'}{R} + \frac{\Theta''}{\Theta} = 0,$$

so each term equals a constant $-n^2$. We obtain the angular ODE and radial ODE

$$\Theta'' + n^2\Theta = 0, \qquad r^2R'' + rR' - n^2R = 0.$$

For integer $n \ge 1$,

$$\Theta(\alpha) = A_n \cos(n\alpha) + B_n \sin(n\alpha),$$

and the radial equation has independent solutions r^n and r^{-n}. Thus the n-th term is

$$r^n\left(C_n \cos n\alpha + D_n \sin n\alpha\right) + r^{-n}\left(E_n \cos n\alpha + F_n \sin n\alpha\right).$$

The $n = 0$ (axisymmetric) case gives Θ = constant and

$$r^2R'' + rR' = 0 \;\Rightarrow\; R(r) = C_0 \ln r + D_0.$$

Putting These Together, the General Solution Is

$$T_b(r,\alpha) = A_0 + B_0 \ln r + \sum_{n=1}^{\infty}\left[r^n\left(A_n \cos n\alpha + B_n \sin n\alpha\right) + r^{-n}\left(C_n \cos n\alpha + D_n \sin n\alpha\right)\right]$$

where the constants A0, B0, An, Bn, Cn, Dn are determined from boundary conditions. If the solution must be finite at the origin (r → 0), all r−n terms and the ln(r) term must be omitted. If the domain is the exterior of a circle and the solution must remain finite as r → ∞, all rn terms and the ln(r) term are omitted. For a problem on an annulus r1 ≤ r ≤r2, both rn and r−n terms generally appear and coefficients are fixed by prescribed values (Dirichlet / Neumann /mixed) on r = r1, r2. This equation is elliptical and may be solved iteratively through the successive over-relaxation method. Once again, no axial flux is considered to occur, so the terms in the z direction have vanished.

Groove Regions

A suitable thermal modeling of the phenomena taking place within groove regions and their surroundings is vital when analyzing the role of feeding conditions. However, within groove regions (recall Fig. C) the thin film assumption (cr « r) which is the basis for the Reynolds equation is no longer valid. A CFD approach could be used, but since this calculation would have to be repeated in each iteration at the expense of massive computation time, a detailed mass and energy balance becomes more appropriate in the scope of the present work. The aim of this balance is to estimate the temperature of the inlet section of the bearing land located downstream of this groove (also called the leading edge of the groove). This temperature will be the initial

condition to be supplied for the resolution of the energy equation at the fluid domain located downstream of that grove. In the present work this balance takes into account: all major inbound and outbound heat fluxes due to lubricant flow across the boundaries of the groove region; the heat fluxes due to forced convection between the bush body and the inner groove lubricant; the influence of the actual groove dimensions, namely the groove length ratio, a/b; the occurrence of fresh oil backflow (upstream of the groove) and reverse flow (downstream of the groove); the influence of the occurrence of negative feeding flow rate (hot oil reflux) in one of the grooves; the existence of a non-uniform temperature profile at the inlet section (leading edge of the groove).

An outline of the heat fluxes crossing the boundaries of the groove region is presented in Fig. E(a). But the thermal balance is not sufficient, by itself, to determine the several average temperatures corresponding to the various outward lubricant flows and the inner groove temperature, gr T. Regardless of the mixing efficiency, it seemed reasonable to assume that the backflow temperature, bkf T and the axial flow temperature axial T will be similar to gr T. However, the average leading-edge temperature will depend on the degree of mixing between the hot oil coming from upstream and reaching the trailing edge of the groove at an average temperature Tavg and the inner groove oil at temperature gr T. An outline of the mixing process is sketched.

in Fig. E (b).

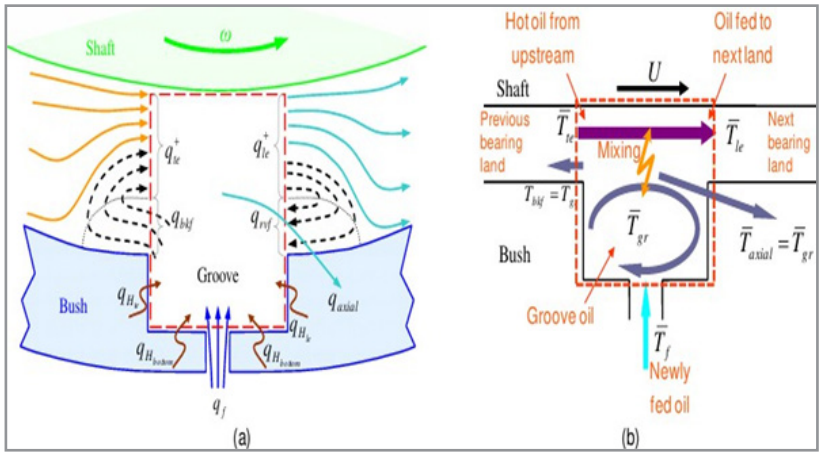

Figure E: (a) Heat fluxes across the boundaries of the groove region in the presence of back flow upstream and reverse flow downstream of the groove; (b) Outline of the thermal mixing model within the groove region. The present thermal approach is 2D, made in the midplane of the bearing, and in fact several studies have confirmed that in most cases the axial temperature gradients along the bearing length are indeed negligible and what happens at the midplane is representative of the whole bearing length. However, if the grooves have a small length, the midplane thermal analysis made above should be corrected in order to reflect, on average, the whole bearing length, and not just the grooved length [23,33]. With the knowledge of the velocity field, it is possible to determine the average inlet section temperature, is T, which reflects more accurately the effective temperature of the whole bearing length.

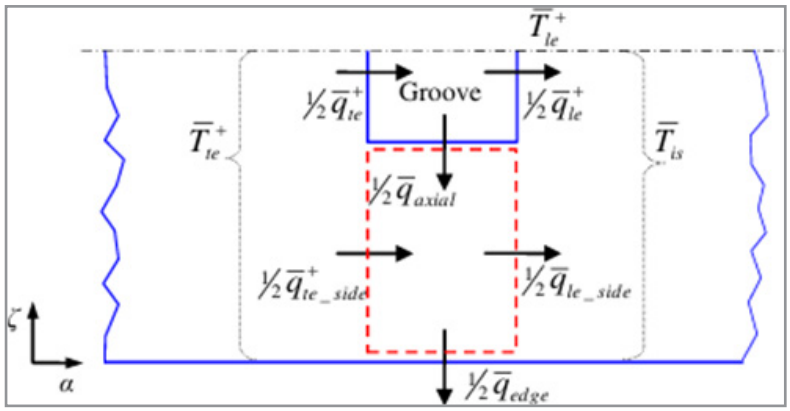

Figure F: Outline of the thermal balance carried out to determine the average inlet section temperature, is T, which incorporates the influence of the groove length ratio, a/b.

Conditions at the Interfaces

At the shaft-film interface a condition of no net heat flux was imposed. This may be considered as a midterm between situations where the shaft acts a heat sink or a heart source. Also, the shaft surface temperature is considered to be constant, following experimental evidence [33]. These two assumptions are widely accepted and used in the literature [34-36]. At the bush-film interface, the temperature and heat flux continuity are applied, while natural and forced convection conditions are used at the bush-ambient interface and at the inner groove walls, respectively. It is worth noting that the accounting for convective heat transfer at the groove walls must be done both in the bush body conduction calculation and in the groove thermal balance. Otherwise, a virtual heat source/sink will exist due to this. A higher

than usual value of 750W/m2K was chosen for Hgr. Such value appears to be in better agreement with the highly recirculating flow found within groove regions and indeed this allowed to replicate the strong temperature fade found experimentally in the vicinity of grooves [24,32,37].

Numerical Procedure

The theoretical model was implemented using the FORTRAN 90/95 programming language. The global algorithm implements the following sequence: Imposition/update of eccentricity and attitude angle, and calculation of the pressure field until attitude angle convergence is achieved; solution of theeach bearing land); solving of the Laplace equation; updating of the bush-film interface temperature and, if it has not converged, going back to the beginning of the thermal algorithm; calculation of the shaft temperature based on the no net heat flux condition and, if this temperature and T is have not converged, going back to the beginning of the thermal algorithm; calculation of the load capacity and, if load has not converged, going back to the beginning of the algorithm, otherwise, conclusion of the calculation. The selection of the mesh parameters and convergence criteria was based on a comprehensive parametric study in order to obtain a good compromise between accuracy and processing time. The approach relied on the use of refined meshes in order to detect more subtle phenomena such as reverse flow.

The two cells in the vicinity of the groove edges were refined by a factor of six after the first little iteration. Taking into account the small randomness found in the results (even at very high eccentricities), along with the small differences found between the results obtained with the final mesh and the finest meshes tested, the present algorithm seems to be particularly robust.

Model Validation

There is a lack of models presenting a thorough validation with experimental data, something which compromises the reliability of the results obtained. Such was tried with the present model. A comparison against the results of, which are extensively used in model validation [38]. A very good theoretical-experimental correlation is obtained for maximum temperature with differences of around 1ºC, within the error of temperature measurements. The temperature trend is fairly well predicted for both cases except in the region immediately downstream of the groove. This may have happened due to the fact that, while the experimental values were measured at the midplane of the bearing, the theoretical approach performs averaged thermal calculations over the whole section. The hydrodynamic pressure profiles displayed in Fig. 7b are within the experimental error margin, the same happening with the estimation of eccentricity ratio. Predicted temperature profiles against experimental results obtained by the authors [39]. Again, it should be highlighted that the temperature correlation in the region immediately downstream of grooves is not satisfactory since the predicted values are representative of the whole section and not just of the midplane, as measured experimentally.

The suitability of the predictions may be better acknowledged by observing the peak temperatures occurring in each one of the bearing lands and also on the shaft surface. In fact, seldom has the temperature trend in the ruptured film region of twin groove journal bearings been accurately predicted. The present model seems to accomplish this rather satisfactorily for the generality of the tests. Comparison between the present analysis and experimental temperature profiles at the midplane of the inner bush surface of the bearing for four different shaft speeds and an applied load of (a) 2kN, (b) 6kN and (c) 10kN; (d) Total flow rate (Pf=140kPa) [39]. Depicts the comparison of the predictions of the present analysis against experimental results from another paper by the group, where the feeding pressure varied threefold from 70 to 210kPa [24]. The same good correlation may be observed (something positive for the present analysis, in the scope of the assessment of feeding conditions), except for the flow rate, which was substantially underestimated. Comparison between theory and experiment, for several loads and shaft speeds, of (a) Shaft surface temperature, (b) maximum bush temperature, (c) maximum bush temperature at the loaded (lower) land and (d) maximum bush temperature at the unloaded (upper) land of the bearing (Pf=140kPa); Unfortunately, the crude underestimation of the flow rate in twin groove journal bearings analyses is a commonly known issue, still unresolved and found in numerous reference works and even popular bearing design tools [8,9,11,34, 39,40].

This might be linked with the intrinsic limitations in the modelling of flow in grooves located in the midst of the ruptured film region and requires further investigation. Nonetheless, this general underestimation does not seem to decisively affect the maximum temperature of the bush, which has been fairly well predicted in most cases. Comparison between theory and experiment, for several loads and feeding pressures, of (a) Shaft surface temperature, (b) maximum bush temperature, (c) maximum bush temperature at the loaded (lower) land, (d) maximum bush temperature at the unloaded (upper) land of the bearing and (e) flow rate. Therefore, the current model seems apt to be used in the analysis of the performance of single and twin groove hydrodynamic journal bearings with realistic feeding conditions [24].

Analysis of Lubricant Feeding Conditions

In continuation, the lubricant feed conditions such as the lubricant feeding pressure and temperature, the groove length ratio (a/b), the groove width ratio (w/d) and the number of grooves (single/twin) are analyzed for a bearing geometry which is roughly the one used in [24,39]. This analysis aims to assess how these parameters may affect bearing performance and how they can be optimized to achieve a reduction in friction without sacrificing the integrity of the system.

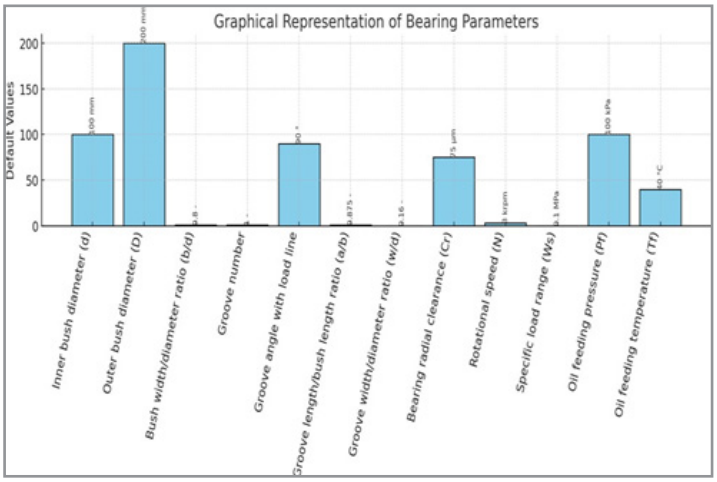

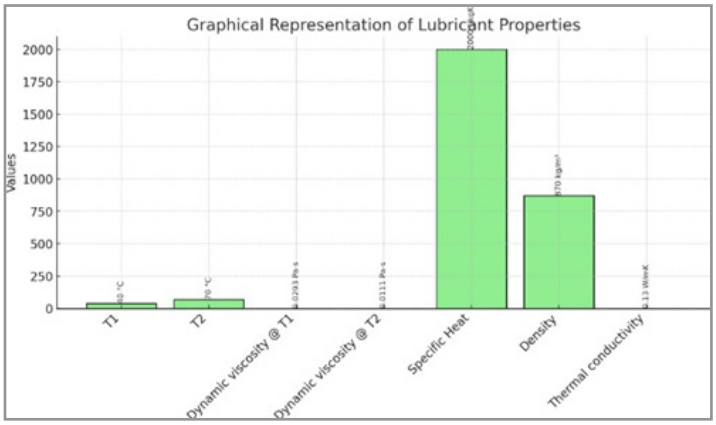

Feeding Pressure (Pf) Feeding pressure (Pf) is one of the feeding parameters which is frequently neglected in modelling as its analysis requires a realistic treatment of groove geometry and a mass conserving algorithm with film rupture and regeneration front estimation. Nonetheless, it affects deeply the thermal behaviour of the bearing due to its cooling effect. Also, if the bearing is too starved, contact might occur, while if there is lubricant excess there will be increased power loss. Effect of Pf on the total flow rate and on the flow rate through each groove, for a broad range of specific loads. While total flow rate follows a well-known trend with load, the flow rates through each groove show rather dissimilar or even opposite trends. This phenomenon has already been observed experimentally and explained in several of the authors' publications, including the curious phenomenon of negative flow rate occurring at high loads in the +90º groove, the groove which serves the loaded land of the bearing (also called the upstream groove) [25-28,42]. This means that this groove starts acting as a lubricant sink instead of a lubricant source for the bearing. This behavior is caused by the excessive closeness between the groove and the strong hydrodynamic pressures, which eventually exceed feeding pressure, reversing pressure gradients and thus the direction of the lubricant flow.

This phenomenon occurs under heavily loaded conditions and thus raises the seizure risk. In fact, the lubricant is being retrieved just upstream of the active bearing region, where it would be most needed. And this lubricant starvation might happen inadvertently since the total flow rate (the parameter which is measured in industrial applications, at best) will indicate a seemingly normal feeding flow rate value. The effect which Pf has on power loss, minimum film thickness (hmin) and maximum bush temperature (Tmax) may be observed in Fig. 12a, b and c, respectively. Indeed, when increasing Pfhmin increases something which is generally positive. However, this is obtained at the expense of an increase in power loss from 9% to 30% for a threefold increase in Pf. This is due to the fact that a higher flow rate of oil will reduce the average oil temperature and thus increase viscosity and viscous drag.

Also, the full film region will be somewhat broader, and so the viscous drag will further increase. By looking at Fig. 12c it can be seen that Tmax is not minimized in the presence of the lowest loads but rather slightly higher values of this parameter. This is due to the fact that lightly loaded bearings typically display a low rate of lubricant leakage/renewal, as observed experimentally [24]. However, it can be observed that an increase in Pf might indeed reduce Tmax significantly for light load conditions. Once increasing Pf from 100kPa to 200 kPa the groove temperature drops abruptly from 64ºC to 42ºC, a value close to the feeding temperature (40ºC). This indicates that the flow rate has started to be positive. Feeding Temperature (Tf) Lubricant viscosity, which strongly depends on temperature, is the parameter responsible for hydrodynamic pressure generation within the fluid. Therefore, the variation of Tf is likely to exert a strong influence not only on the temperature field, the power loss and the flow patterns, but also on minimum film thickness and ultimately on the load carrying capacity of the bearing.

On one hand, if Tf is too low, the viscosity of the lubricant will be high and an excessive power loss will exist. On the other hand, if T+ is too high there will be no sufficient load carrying capacity, with risk of contact. Besides, the thermal crowning of surfaces due to thermal distortion will further raise the risk of seizure. Flow rate data but now as a function of two different

variables, specific load and eccentricity ratio. Within the lower range of specific loads (below 2MPa) the flow rate at the +90º groove increases when Tf rises, indicating the fall on viscosity suffered by the hotter lubricant. However, the opposite occurs for higher specific load values. The reason for this lies in the rise in eccentricity ratio which is much more pronounced for higher loads. In fact, when analyzing this same data, but seen as a function of eccentricity ratio. It is apparent that this latter parameter plays a decisive role in flow rates.

For instance, negative flow rate seems to start occurring for an eccentricity ratio around 0.9 irrespective of the value of Tf. This corresponds to between 8 and 10MPa specific loads, depending on Tf. The increase of eccentricity (or the decrease in minimum film thickness) with increasing Tf may be observed. while the effect of Tf on the maximum temperature and shaft surface temperature as well as power loss is displayed. As expected, the viscosity reduction caused by the increase in Tf with temperature yielded a decrease of the viscous dissipation and, therefore, of the power loss. For instance, a 30% reduction in power loss may be obtained when increasing Tf from 30ºC to 60ºC, for a specific load around 1MPa. In accordance with the experimental observations, the increase in Tmax is always much less than the corresponding increase in Tf: In this case, a 30ºC increase in Tf yielded increases of 7ºC for the lowest load case (Ws =0.1MPa) and 15ºC for the highest (Ws =10MPa) [24, 26].

Another interesting fact is that the increase of Tf triggered the appearance of the hot oil reflux phenomenon in the test withWs=8MPa. Groove Length Ratio (a/b) Despite the present thermal model being 2D (performed in the bearing midplane only), the pressure and flow calculations are performed in the whole 3D fluid domain and the thermal balances of the groove regions (the places where axial temperature differences might be significant) have incorporated the influence of a/b, as noted when describing the model. The hydrodynamic pressure fields obtained for two bearings with dissimilar a/b ratios (0.3 and 0.875). The two different groove geometries can be distinguished by observing their constant pressure plateaus (P=Pf) in groove regions. In the vicinity of the +90º groove and in the region downstream of it, it can be seen that there are some differences between the pressure fields obtained for the two cases: In the case of the large grooved bearing, there is hydrodynamic pressure generation immediately downstream of this groove extending to the whole axial length of the bearing. Groove Width Ratio (w/d) The increase of the circumferential extension of groove, also called the groove width, w, will affect bearing performance in various ways as it reduces the extension of the bush lands and therefore, there will be a loss of load supporting area and load capacity, especially if the grooves are close to the pressure buildup region. However, some caution should be taken with the generalization of these results.

In fact, it has been observed before that the present model tends to over-predict the +90º groove flow rate in the high eccentricity range for the case of the twin groove bearing. This over-estimation might be affecting significantly the predictions in some cases: if in reality and become dominant.

Thermo-Hydrodynamic Model and Findings

A thermo-hydrodynamic (THD) model for the analysis of hydrodynamic journal bearings with realistic lubricant feed conditions was developed to investigate the influence of feeding parameters on bearing performance and friction reduction. The model incorporates the simultaneous solution of the Generalized Reynolds Equation (via a mass-conserving algorithm) and the Energy Equation within the fluid film, coupled with the Laplace equation for heat conduction in the bush body. To ensure realistic representation, the actual groove dimensions were included in the pressure and flow calculations, while models for film rupture and lubricant mixing at grooves were derived. A simplified thermoelastic model was also applied.

Validation and Robustness

The model was validated against experimental data, showing strong agreement with observed trends and robust performance across a wide range of input conditions. Although certain limitations were acknowledged, the results were found to be globally coherent, physically plausible, and characterized by low randomness.

Key Findings

- Feeding Pressure: Increased feeding pressure reduced bearing temperature and prevented hot oil reflux. However, this benefit came at the expense of higher power loss.
- Feeding Temperature: At low loads, elevated lubricant temperature decreased power loss. At high loads, however, it significantly increased eccentricity, maximum temperature (Tmax), maximum pressure (Pmax), and thermal distortions, while lowering the critical load threshold for hot oil reflux.
- Groove Length Ratio (a/b): Smaller groove lengths decreased power loss by ~35%, but reduced cooling efficiency, shortened lubricant film extent, and lowered load- carrying capacity. Excessive reduction risked local contact due to thermal crowning.
- Groove Width Ratio (w/d): Increasing groove width reduced power loss and bush temperature, with minimal effect on load capacity. However, the critical load for hot oil reflux decreased.
- Number of Grooves: Compared to a single groove (+90° to load line), twin grooves (±90°) lowered temperature and eccentricity at high loads. However, they increased power loss and made hot oil reflux more likely at high eccentricities.

Conclusion

The study confirms that lubricant feeding conditions play a vital role in journal bearing performance and must not be overlooked in bearing analyses. Their proper optimization can yield substantial improvements in energy efficiency, thermal stability, and friction reduction. In extreme cases, feeding conditions may determine whether bearing seizure occurs—an aspect conventional design tools cannot reliably predict.

Declarations

Funding

The authors received no financial support for the research, authorship, or publication of this article.

Author Contributions

All authors contributed equally to this work.

Conflict of Interest
The authors declare no conflicts of interest.

Data Availability Statement
The data used in this study were obtained from publicly available online sources.

Institutional Review Board Statement
Not applicable.

Informed Consent Statement
Not applicable.

Ethics Statement
This manuscript does not involve any ethical concerns.

Disclosure of AI Use
Artificial intelligence (AI) tools (e.g., ChatGPT) were used to a limited extent, solely for language refinement and formatting assistance.

References

1. Arab Solghar, A., Brito, F. P., Claro, J. C. P., & Nassab, A. G. (2011). An experimental study of the influence of loading direction on the thermohydrodynamic behavior of twin axial groove journal bearing. Proceedings of the Institution of Mechanical Engineers, Part J: Journal of Engineering Tribology, 225(5), 245–254. https://doi.org/10.1177/1350650111401970.
2. Boncompain, R., Fillon, M., & Frêne, J. (1986). Analysis of thermal effects in hydrodynamic bearings. ASME Journal of Tribology, 108(2), 219–224.
3. Bou Said, B. (1985). La lubrification à basse pression par la méthode des éléments finis: Application aux paliers (Doctoral dissertation, INSA de Lyon, France).
4. Brito, F. P., Bouyer, J., Fillon, M., & Miranda, A. S. (2006). Experimental investigation on the thermal behavior and performance characteristics of a twin axial groove journal bearing as a function of applied load and rotational speed. In Proceedings of the 5th International Conference on Mechanics & Materials in Design (M2D'2006), Porto, Portugal, July 24–26.
5. Brito, F. P., Bouyer, J., Fillon, M., & Miranda, A. S. (2007). Experimental investigation of the influence of supply temperature and supply pressure on the performance of a two axial groove hydrodynamic journal bearing. ASME Journal of Tribology, 129(1), 98–105.
6. Brito, F. P., Miranda, A. S., Claro, J. C. P., & Fillon, M. (2007). The role of each groove on the behavior of twin axial groove journal bearings. In IBERTRIB - Congreso Ibérico de Tribología, Bilbao, Spain, June 20–21.
7. Brito, F. P., Miranda, A. S., Claro, J. C. P., & Fillon, M. (2011). The role of lubricant supply temperature on the performance of twin groove journal bearings: An experimental study. International Journal of Surface Science and Engineering, 5(4), 286–299. https://doi.org/10.1504/IJSURFSE.2011.044278.
8. Brito, F. P., Miranda, A. S., Claro, J. C. P., & Fillon, M. (2012). Experimental comparison of the performance of a journal bearing with a single and a twin axial groove configuration. Tribology International, 54, 1–8.
9. Brito, F. P., Miranda, A. S., Claro, J. C. P., Teixeira, J. C., Costa, L., & Fillon, M. (2012). On the occurrence of negative groove flow rate in twin groove hydrodynamic journal bearings. In Proceedings of the 15th International Conference on Experimental Mechanics (ICEM15), Porto, Portugal, July 22–27 (pp. 875–876).
10. Chun, S., & Lalas, D. (1992). Parametric study of inlet oil temperature of a half-circumferential grooved journal bearing. STLE Tribology Transactions, 35(2), 213–224.
11. Claro, J. C. P., & Miranda, A. S. (1993). Analysis of hydrodynamic journal bearings considering lubricant supply conditions. Proceedings of the Institution of Mechanical Engineers, Part C: Journal of Mechanical Engineering Science, 207(C3), 183–194.
12. Costa, L., Fillon, M., Miranda, A. S., & Claro, J. C. P. (2003). An analysis of the influence of oil supply conditions on the thermohydrodynamic performance of a single groove journal bearing. Proceedings of the Institution of Mechanical Engineers, Part J: Journal of Engineering Tribology, 217(2), 133–144.
13. Costa, L., Fillon, M., Miranda, A. S., & Claro, J. C. P. (2003). An experimental investigation of the effect of groove location and supply pressure on the THD performance of a steadily loaded journal bearing. ASME Journal of Tribology, 122(2), 227–232.
14. Dowson, D., Hudson, J., Hunter, B., & March, C. (1966–1967). An experimental investigation of the thermal equilibrium of steadily loaded journal bearings. Proceedings of the Institution of Mechanical Engineers, Part 3B, 101, 70–80.
15. Dowson, D., Taylor, C. M., & Miranda, A. S. (1985). The prediction of liquid film journal bearing performance with a consideration of lubricant film reformation, Part I & II. Proceedings of the Institution of Mechanical Engineers, 119(C2), 95–102, 102–111.
16. El-Deihi, M. K. I., & Gethin, D. T. (1992). A thermohydrodynamic analysis of a twin axial groove bearing under different loading directions and comparison with experiment. ASME Journal of Tribology, 114(2), 304–310.
17. Elrod, H. G. (1981). A cavitation algorithm. ASME Journal of Lubrication Technology, 103(3), 350–354.
18. Ferron, J., Frêne, J., & Boncompain, R. (1983). A study of the thermohydrodynamic performance of a plain journal bearing: Comparison between theory and experiments. ASME Journal of Lubrication Technology, 105(3), 422–428.
19. Fitzgerald, M. K., & Neal, P. B. (1992). Temperature distributions and heat transfer in journal bearings. ASME Journal of Tribology, 114(1), 122–130.
20. Gethin, D. T., & El-Deihi, M. K. I. (1990). Thermal behavior of a twin axial groove bearing under varying loading direction. Proceedings of the Institution of Mechanical Engineers, Part C: Journal of Mechanical Engineering Science, 204(C1), 77–90.
21. Groper, M., & Etsion, I. (2002). Reverse flow as a possible mechanism for cavitation pressure build-up in a submerged journal bearing. ASME Journal of Tribology, 124(2), 320–326.
22. Heshmat, H. (1991). The mechanism of cavitation in hy-

drodynamic lubrication. Tribology Transactions, 34(2), 177–186.
23. Jang, J. Y., & Khonsari, M. M. (2004). Design of bearings on the basis of thermohydrodynamic analysis. Proceedings of the Institution of Mechanical Engineers, Part J: Journal of Engineering Tribology, 218(3), 355–363.
24. Jeddi, L., El Khlifi, M., & Bonneau, D. (2005). Thermohydrodynamic analysis for a hydrodynamic journal bearing groove. Tribology International, 38(3), 263–274.
25. Keogh, P. S., & Khonsari, M. M. (2001). Influence of inlet conditions on the thermohydrodynamic state of a fully circumferentially grooved journal bearing. ASME Journal of Tribology, 123(3), 525–532.
26. Knight, J. D., & Ghadimi, P. (1992). Effects of modified effective length models of the rupture zone on the analysis of fluid journal bearings. STLE Tribology Transactions, 35(1), 29–36.
27. Knight, J. D., & Ghadimi, P. (2001). Analysis and observation of cavities in a journal bearing considering flow continuity. STLE Tribology Transactions, 44(1), 88–96.
28. Knight, J. D., Barret, L., & Cronan, R. D. (1985). The effects of supply pressure on operating characteristics of two-axial groove bearings. STLE Tribology Transactions, 28(3), 336–342.
29. Kosasih, P. B., & Tieu, A. K. (2004). An investigation into the thermal mixing in journal bearings. Proceedings of the Institution of Mechanical Engineers, Part J: Journal of Engineering Tribology, 218(4), 379–389.
30. Lund, J. W., & Tonnesen, J. (1984). An approximate analysis of the temperature conditions in a journal bearing: Part II – Application. ASME Journal of Tribology, 106(2), 237–245.
31. Ma, M. T., & Taylor, C. M. (1992). A theoretical and experimental study of thermal effects in a plain circular steadily loaded journal bearing. In IMechE Seminar: Plain Bearings – Energy Efficiency and Design (pp. xx–xx). Mechanical Engineering Publications Ltd.
32. Ma, M. T., & Taylor, C. M. (1994). Prediction of temperature fade in cavitation region of two-lobe journal bearings. Proceedings of the Institution of Mechanical Engineers, Part C: Journal of Mechanical Engineering Science, 208(C2), 133–139.
33. Ma, M. T., & Taylor, C. M. (1995). Effects of oil temperature on the performance of an elliptical bearing. In Proceedings of the 21st Leeds-Lyon Symposium on Tribology, Tribology Series (Vol. 30, pp. 143–151).
34. Pierre, I., & Fillon, M. (2000). Influence of geometric parameters and operating conditions on the thermohydrodynamic behavior of plain journal bearings. Proceedings of the Institution of Mechanical Engineers, Part J: Journal of Engineering Tribology, 214(5), 445–457.
35. Pierre, I., Bouyer, J., & Fillon, M. (2004). Thermohydrodynamic behavior of misaligned plain journal bearings: Theoretical and experimental approaches. Tribology Transactions, 47(4), 594–604.
36. Pinkus, O. (1990). Thermal aspects of fluid film tribology. ASME Press.
37. Rajalingham, C., & Prabhu, B. S. (1987). The influence of variation of viscosity with temperature on the steady-state characteristics of journal bearings: Simple analysis. Tribology International, 20(5), 261–266.
38. Tonnesen, J., & Hansen, P. K. (1981). Some experiments on the steady-state characteristics of a cylindrical fluid film bearing considering thermal effects. ASME Journal of Lubrication Technology, 103(1), 107–114.
39. Vijayaraghavan, D. (1996). An efficient numerical procedure for thermohydrodynamic analysis of cavitating bearings. ASME Journal of Tribology, 118(3), 555–563.
40. Vijayaraghavan, D., Keith, T. G., Jr., & Brewe, D. E. (1996). Effect of lubricant supply starvation on the thermohydrodynamic performance of a journal bearing. Tribology Transactions, 39(3), 645–653.